

5.3. Amundsen-Scott South Pole Station (1/28/04–1/17/05)

The 2004-2005 season at Amundsen-Scott South Pole Station is defined as the period between the site visits 1/20/04–1/30/04 and 1/18/05–1/24/05. The season opening and closing calibrations were performed on 1/27/04 and 1/18/05, respectively. Volume 14 solar data comprise the period 1/28/04–1/17/05. About 90% of the scheduled scans are part of the data set; 5.2% are missing because of technical problems.

Except of the issues described in the following, the system performed well:

- **Failure of system control computer**

The system control computer failed on 12/3/04 and was replaced by the spare computer on 12/5/04. A new computer was sent to the South Pole and installed on 1/3/05.

- **Change of responsivity**

The system's responsivity changed by 10% between 7/22/04 and 8/25/04. The reason for this change could not be identified. Solar data are not affected since the problem occurred during Polar Night.

- **GUV malfunction**

The GUV-541 radiometer did not work when it was reinstalled after Polar Night. The problem was caused by a defective cable. The cable was repaired and later replaced by a new cable with better low-temperature rating. This problem lead to some data loss.

The Eppley PSP instrument installed at South Pole was replaced by identical instruments during the site visits in 2004 and 2005. The instrument installed during the Volume 14 period had been calibrated by Eppley Laboratory in March 2003.

5.3.1. Irradiance Calibration

The site irradiance standards for the 2004/05 South Pole season were the lamps 200W006, 200W021, and M-666. Lamp M-764 was used as the traveling standard at the beginning and end of the season. The lamp has been re-calibrated by Optronic Laboratories in March 2001.

Lamp 200W021 has an irradiance calibration of Optronic Laboratories from September 1998. Lamp 200W006 was originally calibrated by Optronic Laboratories in November 1996. The lamp was dropped during the site visit in 2004 and recalibrated against M-764 using data from 1/28/04. The lamp proved to be stable during the 2004/05 season despite the mechanical stress that it had suffered. Lamp M-666 was calibrated with lamps 200W006 and 200W021 using season closing scans of Volume 9 and opening scans of Volume 10. See Section 4.2.1.5. for further details on the method of transfer.

Figure 5.3.1 shows a comparison of lamps 200W006, 200W021, and M-666 with M-764 at the start of the season (1/28/04). The figure indicates that all lamps agreed with M-764 to within $\pm 1.5\%$. Figure 5.3.2 shows a similar comparison for the end of the season. At this time, all lamps agreed to within $\pm 2\%$.

Lamps 200W006, 200W021, and M-666 were additionally compared against each other shortly before and after Polar Night and agreed to within $\pm 2\%$.

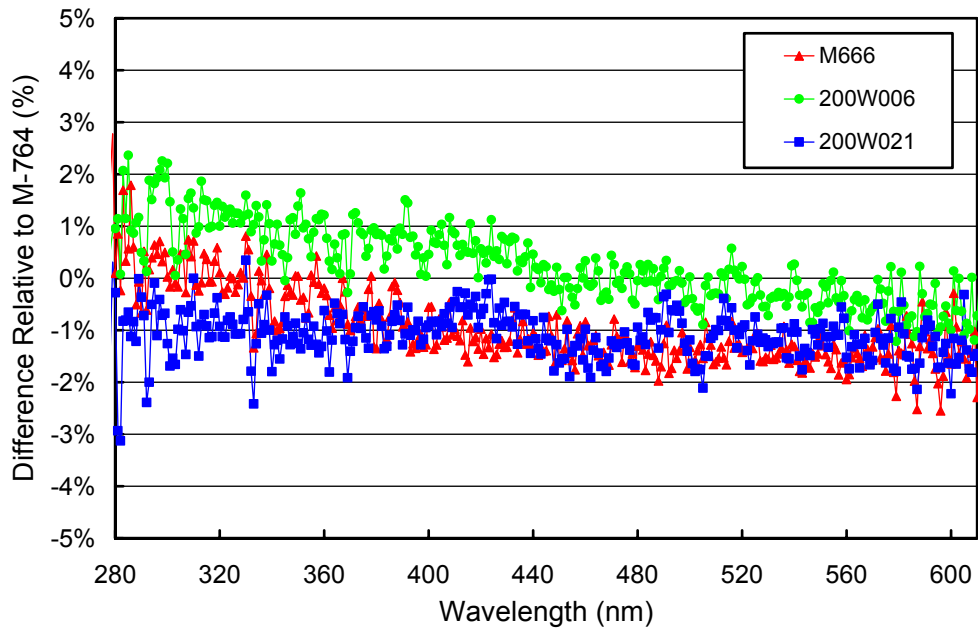


Figure 5.3.1. Comparison of South Pole lamps 200W006, 200W021, and M-666 with the BSI traveling standard M-764 at the start of the season on 1/27/04 and 1/28/04

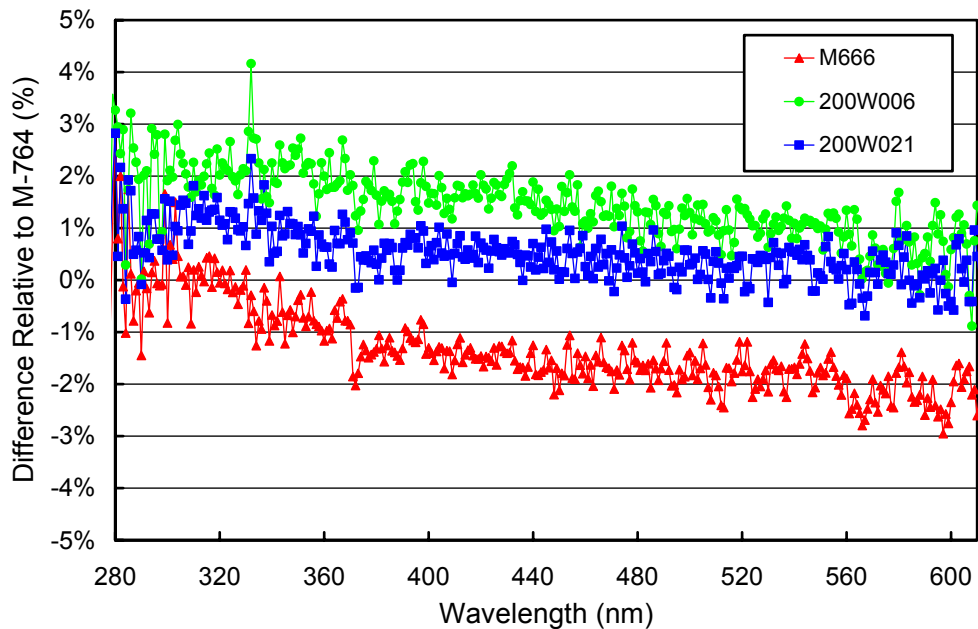


Figure 5.3.2. Comparison of South Pole lamps 200W006, 200W021, and M-666 with the BSI traveling standard M-764 at the end of the season on 1/18/05.

5.3.2. Instrument Stability

The stability of the spectroradiometer over time is primarily monitored with bi-weekly calibrations utilizing site irradiance standards, and daily response scans of the internal irradiance reference lamp. The stability of the internal lamp is monitored with the TSI sensor, which is independent from possible monochromator and PMT drifts.

Figure 5.3.3 shows the changes in TSI readings and PMT currents at 300 and 400 nm, derived from the daily scans of the internal lamp during the South Pole 2004/05 season. The TSI measurements indicate that the internal lamp became brighter by about 2% during the year. This amount of drift is typical. The PMT currents at 300 and 400 nm are approximately tracking the signal of the TSI, except for a period between 7/22/04 and 8/25/04 when PMT currents were high by 10%. During this period, the temperature of the roofbox was being optimized by the research associate. However, this adjustment should not have changed the system responsivity by this amount and the actual reason for change is unknown. The problem has no impact on solar data since it occurred during Polar Night.

A total of five different calibrations were applied to the solar measurements of Volume 14. An overview of the calibration periods is given in Table 5.3.1. Figure 5.3.4 shows ratios of the calibration functions applied during Periods 2-5, relative to the function of Period 1. Differences between two consecutive calibration periods are generally less than 2%, except for the break between Periods P2 and P3, which are separated by the Polar Night.

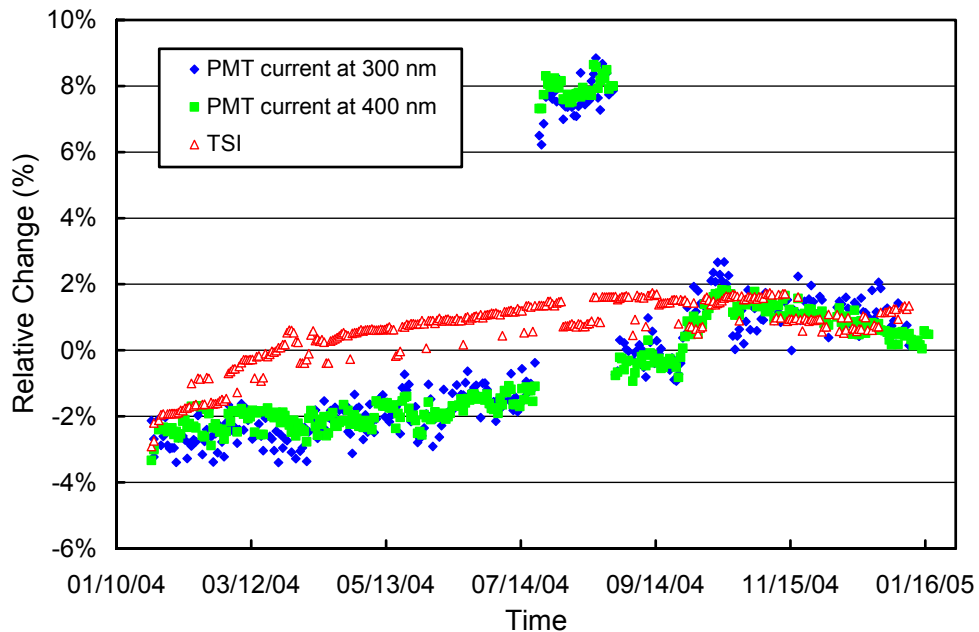


Figure 5.3.3. Time-series of PMT current at 300 and 400 nm, and TSI signal during measurements of the internal irradiance standard performed during the South Pole 2004/05 season. The data are normalized to the average of the whole period.

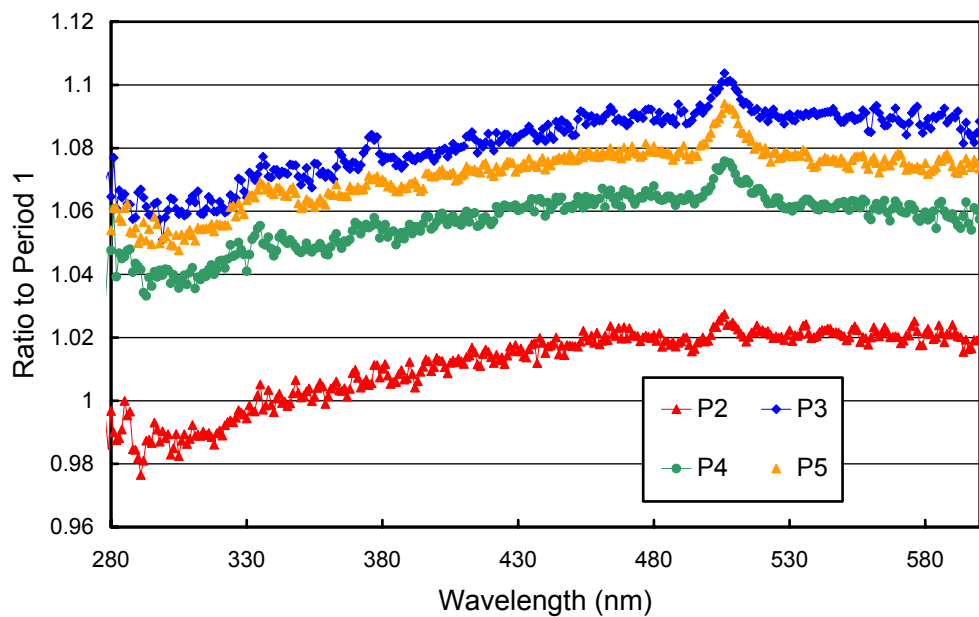


Figure 5.3.4. Ratios of irradiance assigned to the internal lamp relative to Period 1.

Figure 5.3.5 presents the relative standard deviation calculated from the individual calibration scans of each period. These data are useful for estimating the variability of the calibrations in each period. The variability is typically less than 1.5% for wavelengths above 300 nm in all periods, indicating good stability.

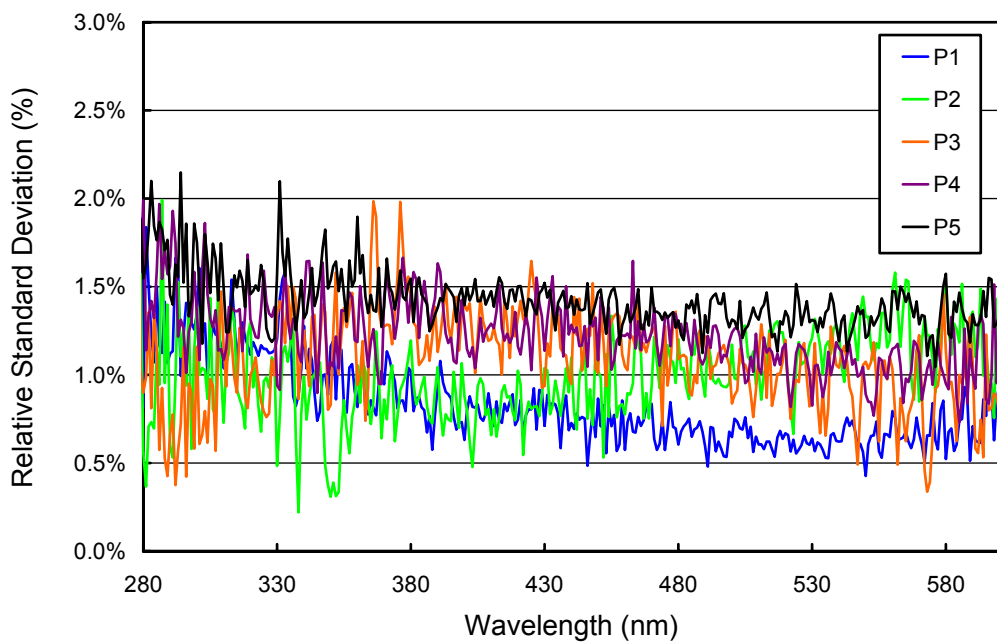


Figure 5.3.5. Relative standard deviation calculated from the absolute calibration scans measured during the South Pole 2004/05 season.

Table 5.3.1. Calibration periods for South Pole Volume 14 data.

Period name	Period range	Number of Absolute scans	Remarks
P1	01/22/04 - 03/04/04	11	
P2	03/05/04 - 06/21/04	4	Before Polar Night
P3	06/22/04 - 10/06/04	4	After Polar Night
P4	10/07/04 - 12/04/04	6	
P5	12/05/04 - 01/19/05	12	

5.3.3. Wavelength Calibration

Wavelength stability of the system was monitored with the internal mercury lamp. Information from the daily wavelength scans was used to homogenize the data set by correcting day-to-day fluctuations in the wavelength offset. After this step, there may still be a deviation from the correct wavelength scale, but this bias should be similar for all days. Figure 5.3.6 shows the difference of the wavelength offset of the 296.73 nm mercury line between two consecutive wavelength scans. In total, 392 scans were evaluated. The change in offset was smaller than ± 0.025 nm for 86% of the scans and smaller than ± 0.055 nm for 97% of the scans. The shifts between 10 scan-pairs was larger than ± 0.1 nm due to operator intervention or system service; the wavelength calibration was adjusted accordingly.

After the data was corrected for day-to-day wavelength fluctuations, the wavelength-dependent bias between this homogenized data set and the correct wavelength scale was determined with the Fraunhofer-correlation method, as described in Section 4.2.2.2. The resulting correction function is shown in Figure 5.3.7. The corrections exceed 1 nm for wavelengths larger than 500 nm. The magnitude of the correction is considerably larger than typical and is caused by the monochromator installed. As this correction is well defined, accuracy of solar data is not compromised.

After the data has been wavelength corrected using the shift-function described above, the wavelength accuracy was tested again with the Fraunhofer method. The results are shown in Figure 5.3.8 for four UV wavelengths. The residual shifts are typically smaller than ± 0.05 nm. The somewhat larger scatter shortly before and after Polar Night is caused by low light levels, which affect the precision of the correlation algorithm. The actual wavelength uncertainty of the instrument may be slightly larger as indicated in Figure 5.3.8 due to wavelength fluctuations during a given day (Figure 5.3.8 shows only one point per day), and possible systematic errors of the Fraunhofer-correlation method (Section 4.2.2.2).

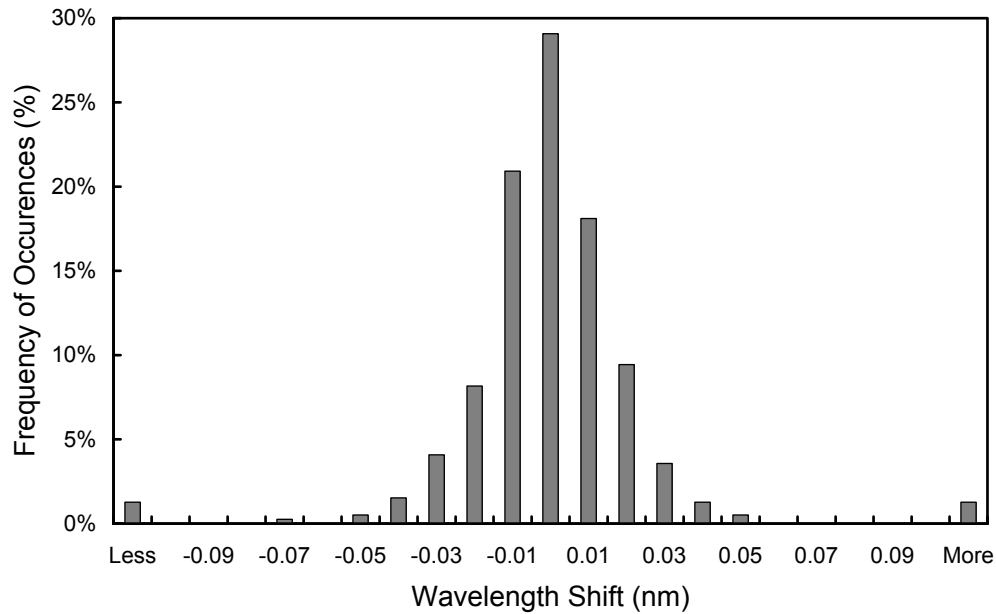


Figure 5.3.6. Frequency distribution of the difference of the measured position of the 296.73 nm mercury line between consecutive wavelength scans. The x-labels give the center wavelength shift for each column. The 0-nm histogram column covers the range -0.005 to +0.005 nm. “Less” means shifts beyond -0.105 nm; “more” means shifts beyond +0.105 nm.

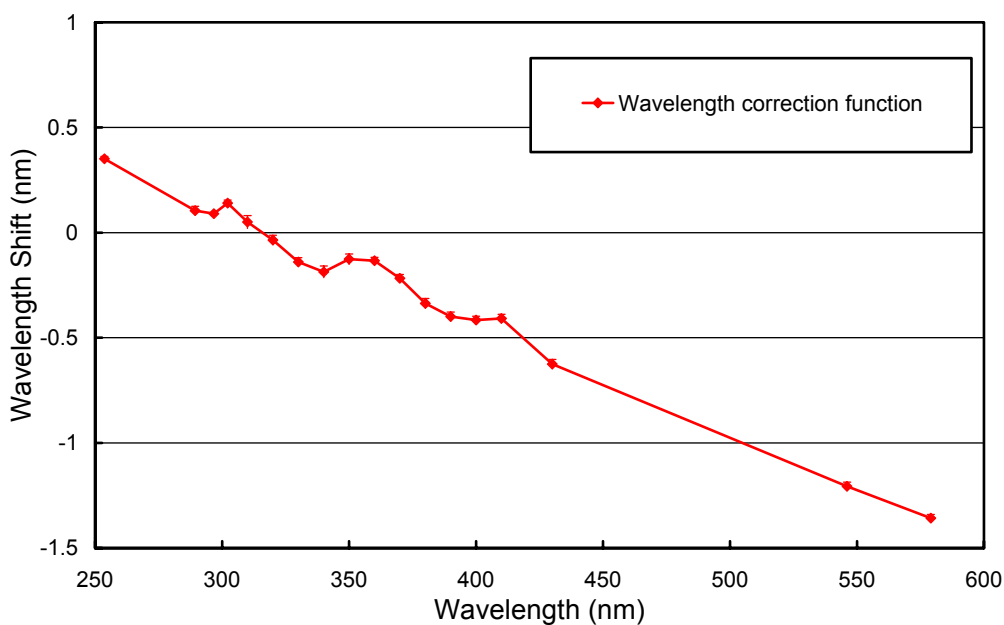


Figure 5.3.7. Monochromator non-linearity functions for the South Pole 2004/05 season.

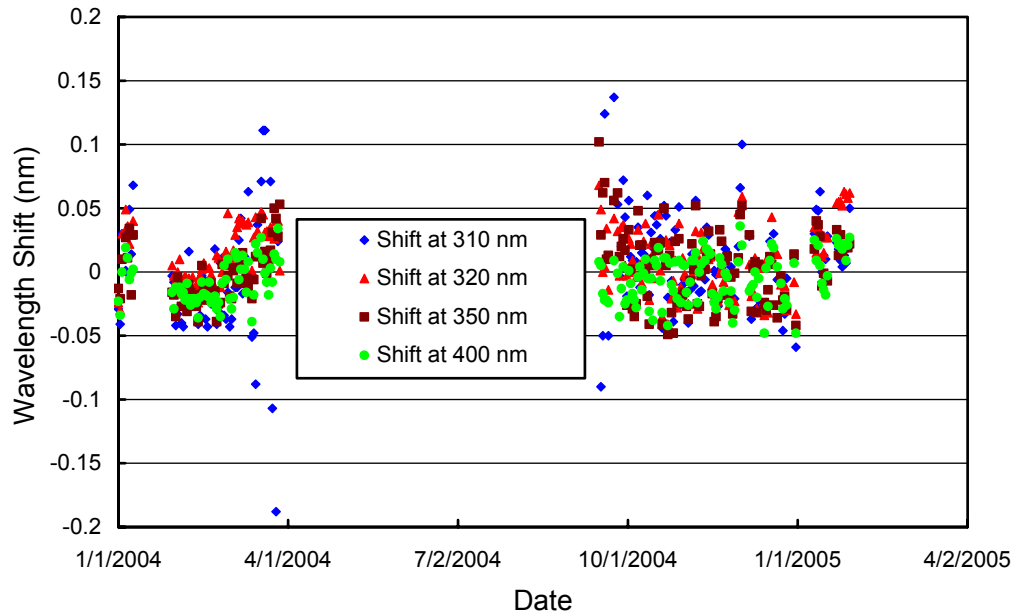


Figure 5.3.8. Wavelength accuracy check of the final data at four wavelengths by means of Fraunhofer correlation. The noontime measurement has been evaluated for each day of the season. No data exist during Polar Night.

Although data from the external mercury scans do not have a direct influence on data products, they are an important part of instrument characterization. Figure 5.3.9 illustrates the difference between internal and external mercury scans collected during both site visits. External scans have a bandwidth of about 1.06 nm FWHM and internal scans of 0.74 nm FWHM. The center wavelengths are shifted by about 0.08 nm. The reason for this discrepancy is explained in Section 4. Since external scans have the same light path as solar measurements, they represent the monochromator bandpass relevant for solar scans more realistically. Figure 5.3.9 indicates that scans performed during the sites visits in 2004 and 2005 are very consistent.

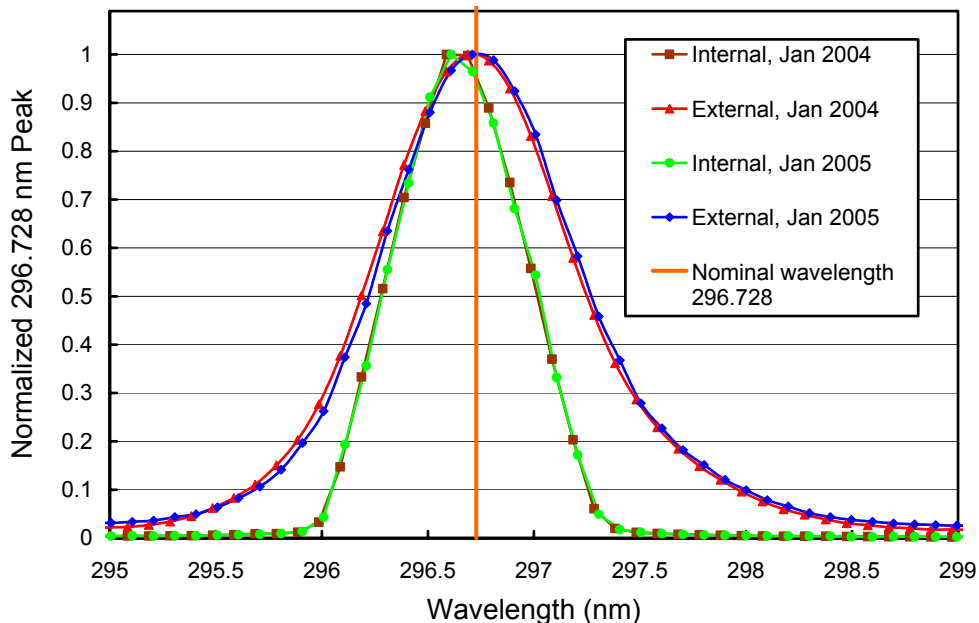


Figure 5.3.9. The 296.73 mercury line as registered by the PMT from external and internal sources.

5.3.4. Missing Data

A total of 15848 scans are part of the published South Pole Volume 14 dataset. These are about 90% of all scans scheduled. Of the missing scans, 76, 400, and 298 were superseded by absolute, wavelength, and response scans, respectively. Since South Pole Station has 24 hours of sunlight per day during the summer season, a loss of solar data cannot be avoided. Because of technical problems, 5.2% of the scheduled scans are missing: a total of 286 scans were lost between 12/03/04 and 12/05/04, when the system control computer became defective and had to be replaced by the spare computer. This computer "hang" for unknown reasons on 12/12/04 and 12/13/04, causing a loss of 117 scans. The computer was also unresponsive on 12/27/04 and 12/28/04, possibly triggered by a anti-virus scan and 122 scans were not recorded. When the spare computer was replaced by a new computer on 1/4/05 and 1/5/05, 79 scans were lost. Reading the instrument's GPS receiver frequently prevented the next scan to run, causing a total loss of 256 scans throughout the season. Work aimed to improved the system's temperature stability conducted on 9/24/04 and 9/25/04 lead to a loss of 38 scans. Due to operator intervention, installation of computer security patches, and other system service 49 scans were not recorded. 37 additional scans were excluded from the data set that were affected by shade from the air sampling stack installed at the ARO building.

5.3.5. GUV Data

The GUV-511 radiometer installed next to the SUV-100 was calibrated against final SUV-100 measurements following the procedure outlined in Section 4.3.1. Data products were calculated from the calibrated measurements (Section 4.3.2). Figure 5.3.10. shows a comparison of GUV-541 and SUV-100 erythemal irradiance. Both data sets agree to within $\pm 4\%$ for solar zenith angles up to 80° , with few exceptions. This good agreement is also indicative of the consistency of the SUV-100 data set. There are some gaps in the GUV-541 time series. The GUV-541 radiometer did not work when it was reinstalled after Polar Night. The problem was caused by a defective cable. The cable was provisionally repaired, but there were still intermittencies between 9/28/04 – 10/4/04 and 10/28/04 – 11/4/04. In addition, GUV measurements are not available for the period when the spare computer was installed (12/2/04 – 1/4/05). On 1/4/05, a new computer was installed and the defective GUV cable was replaced by one with better low-temperature rating. No problems were encountered thereafter.

The agreement for some data products (e.g. DNA damaging variation) may be worse than that for erythemal irradiance due to principal limitations in calculating dose-rates from the five GUV-541 channels when the Sun is low and when the data product in question is heavily weighted toward wavelengths below 310 nm. We therefore advise data users to use SUV-100 rather than GUV-541 data when possible, in particular for low-Sun conditions.

Figure 5.3.11 shows a comparison of total ozone measurements from the GUV-541 and NASA/TOMS Earth Probe satellite (Version 8). GUV-511 ozone values were calculated as described in Section 4.3.3. Both data sets agree reasonably well, but the agreement is somewhat depending on the total ozone column. For solar zenith angles larger than 80° , GUV-541 data become unreliable and should not be used. Differences between the two data sets can partly be attributed to the fact that the look-up table used for GUV-541 ozone determination was calculated with an ozone profile for medium ozone depletion and is not appropriate for periods with very low ozone, such as the period between 11/4/04 – 11/14/04.

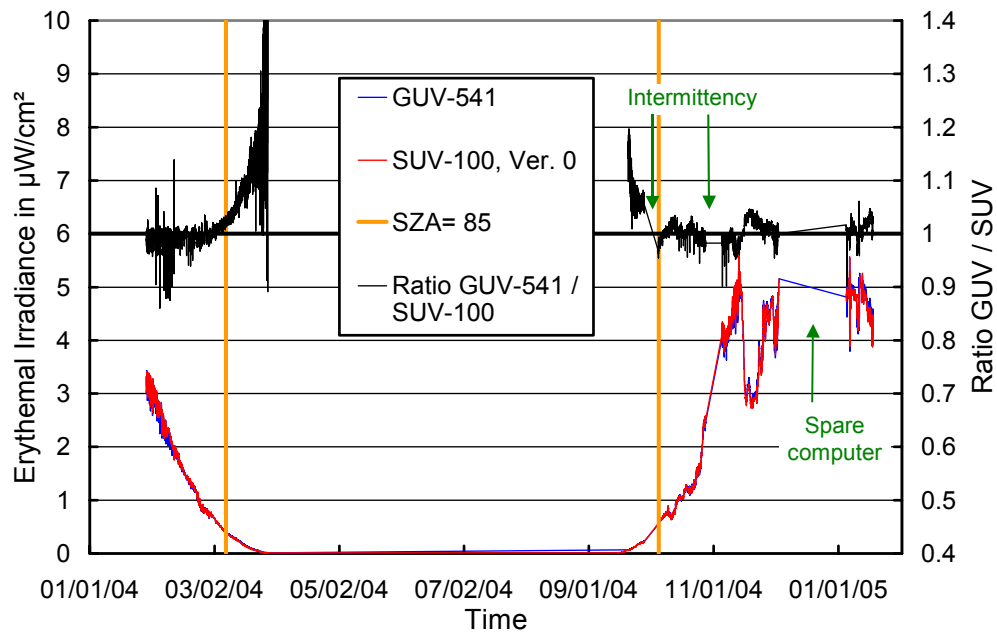


Figure 5.3.10. Comparison of erythemal irradiance measured by the SUV-100 spectroradiometer and the GUV-541 radiometer.

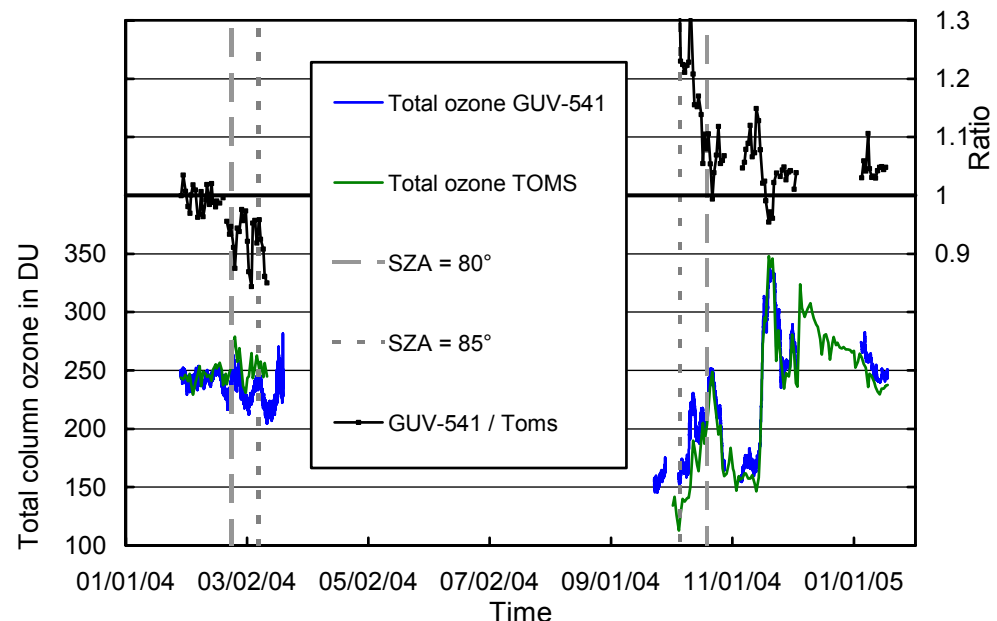


Figure 5.3.11. Comparison of total column ozone measurements from GUV-541 and NASA/TOMS Earth Probe satellite.